Experimental high Reynolds number turbulence with an active grid

Nicolas Mordant

Citation: American Journal of Physics **76**, 1092 (2008); doi: 10.1119/1.2980582
View online: https://doi.org/10.1119/1.2980582
View Table of Contents: https://aapt.scitation.org/toc/ajp/76/12
Published by the American Association of Physics Teachers

ARTICLES YOU MAY BE INTERESTED IN

Decay of homogeneous, nearly isotropic turbulence behind active fractal grids
Physics of Fluids **26**, 025112 (2014); https://doi.org/10.1063/1.4865232

Optimizing the performance of an active grid to generate high intensity isotropic free stream turbulence
Physics of Fluids **32**, 095120 (2020); https://doi.org/10.1063/5.0018932

The puzzle of the steady-state rotation of a reverse sprinkler
American Journal of Physics **83**, 296 (2015); https://doi.org/10.1119/1.4901816

On the probability distribution function of the velocity field and its derivative in multi-scale turbulence
Physics of Fluids **23**, 095106 (2011); https://doi.org/10.1063/1.3632090

Flight and bounce of spinning sports balls
American Journal of Physics **88**, 934 (2020); https://doi.org/10.1119/10.0001659

Stirring turbulence with turbulence
Physics of Fluids **27**, 125107 (2015); https://doi.org/10.1063/1.4937427

AAPT PHYSICS EDUCATION®

Advance your teaching and career
as a member of AAPT

LEARN MORE

Experimental high Reynolds number turbulence with an active grid

Nicolas Mordant[a)]
Laboratoire de Physique Statistique, Ecole Normale Supérieure, 24 rue Lhomond, F-75005 Paris, France

(Received 11 April 2008; accepted 19 August 2008)

This article describes the wind tunnel used in the Physics Department of the Ecole Normale Supérieure in Paris for undergraduate laboratory courses. By using an active grid, which consists of a grid of shafts fitted with randomly rotating wings, a fully turbulent flow is observed. The velocity of the air flow is measured with a low cost hot wire probe. The Reynolds number is large enough so that predictions of the 1941 Kolmogorov theory of turbulence can be observed, such as the famous $k^{-5/3}$ spectrum, in spite of the small size of the tunnel. Deviations from the Kolmogorov theory are also observed and quantified. The moderate cost and size of the wind tunnel due to the use of the active grid make it a valuable teaching tool for introducing the phenomenology of turbulence to undergraduates. © *2008 American Association of Physics Teachers.*
[DOI: 10.1119/1.2980582]

I. INTRODUCTION

Air and water are the ubiquitous fluids of human life. Flows of these fluids in a coffee cup (and at smaller sizes) and in the atmosphere are usually turbulent. From a theoretical point of view, turbulence remains a mystery, even though the Navier-Stokes equation describing fluid motion has been known for about a century and a half. The difficulty is not the equations, but their solutions. A breakthrough occurred in 1941 with the publication of Kolmogorov's phenomenological theory. For a review of the theoretical aspects of turbulence, the reader should refer to Ref. 1.

In this paper I will discuss a relatively small wind tunnel that was built at the Department of Physics of the Ecole Normale Supérieure in Paris for undergraduate laboratory courses. The difficulty of a turbulence experiment is reaching a high enough turbulence so that the basic hypotheses of the Kolmogorov theory are satisfied. Among these is scale separation. The energy input into the flow at large scales of order L (the integral length scale) is transferred by nonlinear terms of the Navier-Stokes equation from large length scales down to small length scales at which the velocity gradients are large enough to be dissipated by viscosity (the traditional cascade picture). A characteristic length scale of this dissipative range is the Kolmogorov length scale, which is usually noted by η. The Kolmogorov theory assumes that η and L are widely separated so that an inertial range exists in between the two where the Kolmogorov theory is applicable.

In classical, grid generated, wind tunnel turbulence a large wind tunnel is required (typically 1 m wide and 10 m long) together with very high speeds (25 m/s) which are beyond the capacity of a typical teaching physics laboratory. Recently, a new and efficient way to generate high levels of turbulence in small wind tunnels has been developed using active grids. These active grids open the possibility of a reasonable size wind tunnel for teaching and even research with the Reynolds number high enough to observe features of fully developed turbulence. Our wind tunnel is about 4 m long with a cross section of 25×25 cm^2.

I will first describe the experimental setup. Then I will present measurements performed in the wind tunnel. I will show that our moderate size wind tunnel reaches high enough Reynolds numbers to test a few predictions of the theory of homogeneous and isotropic turbulence, including the famous $k^{-5/3}$ spectrum. Then I will describe observed deviations from the Kolmogorov theory and show that our measurements agree very well with commonly accepted observations.

II. DESCRIPTION OF THE WIND TUNNEL

A picture of the wind tunnel is in Fig. 1. It is composed of several sections made of 1 cm thick plywood. Four 37 W fans (EBMPAPST model DV6224) suck the air into the tunnel. The next section narrows because the fans are too big to fit in the 25 cm width of the tunnel. The next section is 1 m long and ends with a 8 cm thick honeycomb (with holes 3 mm in diameter) for damping the vortices generated by the fans. After this section the flow is rather homogeneous with fluctuations of the order of 2% of the mean velocity, which can reach 7.5 m/s at the full speed of the fans (without the active grid). Air then flows through the active grid system followed by a 2 m test section with a free exit. The test section has Altuglas windows on one side with a slit at mid-height to enable the positioning of a probe inside the wind tunnel.

The active grid was introduced by Makita[2] and is valuable for turbulence studies because the level of velocity fluctuations and the integral length scale are larger than a conventional static grid. The isotropy of the turbulent fluctuations can be controlled to some extent by the driving scheme of the grid. The principle of the active grid is the following: each rod of the grid is equipped with wings and is free to rotate. It is driven by its own motor whose direction and rotation frequency can be changed during operation. An extensive study of the driving of the grid and its impact on the flow has been done by Poorte and Biesheuvel.[3] We built a grid with five rods in the vertical and horizontal direction (see Fig. 2). Each motor direction is controlled by an independent logic signal from a PCI-6281 National Instrument DAQ card. There are also eight independent TTL clock signals issued from another PCI-6221 card. The eight clocks are connected to the ten motors (two pairs of motors share the same clock line because of technical limitations).

A typical driving mode is the following: the direction is flipped after a time randomly chosen in the interval [1,2.5] s. The rotation rate is changed at a random time chosen in the interval [1,2] s and the new rotation rate is chosen in the interval [2.1,3.75] Hz. The process is independent for each rod and is repeated indefinitely. This forcing mode has

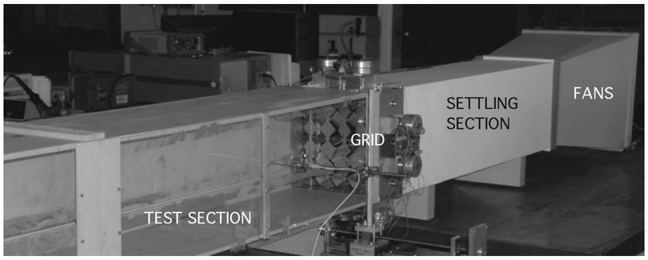

Fig. 1. View of the wind tunnel at the Department of Physics of Ecole Normale Supérieure. Four fans (in the right part) suck the air into the tunnel. A 1 m long settling section with honeycomb parts damps the vortices generated by the fans. The active grid (middle of the picture) is followed by a 2 m long test section. The overall length is about 3.5 m long in this configuration. The cross section is 25×25 cm^2.

been found to yield the ratio of the transverse to longitudinal velocity fluctuations close to 0.925 (measured with a laser Doppler velocimetry system from TSI). This ratio holds from about 50 cm of the grid to the exit of the wind tunnel.

The classical tool for velocity measurements in wind tunnels is the hot wire probe (we use a single wire probe model 55P16 coupled to a Mini-CTA 54T30 from Dantec Dynamics). Its principle is very simple: when you blow on a hot object, it cools. A very thin metal wire is heated by an electrical current (through the Joule effect). The temperature is directly related to its resistance because the latter is a linear function of the temperature for metal wires. When air is blown on the wire, a closed loop system maintains its resistance constant and outputs the required voltage. This voltage is a function of the velocity. The hot wire is sensitive mainly to the magnitude $u_\perp$ of the velocity orthogonal to the wire so that it is positioned orthogonally to the main flow when a single probe is used; more complex configurations can be operated with several wires. Let us assume that the dominant component of the velocity is $u_x \gg (u_y, u_z)$ with $u_x > 0$ (a strong average wind along the x direction with small fluctuations), and that the wire is along the z direction. The magnitude of the perpendicular velocity is $u_\perp \simeq u_x(1+u_y^2/2u_x^2)$ to lowest order in u_y/u_x. The wire is thus sensitive mostly to the velocity component u_x along the average velocity if the fluctuations are not too strong. Here u_y/u_x is about 20% so that the correction is of a couple of percent.

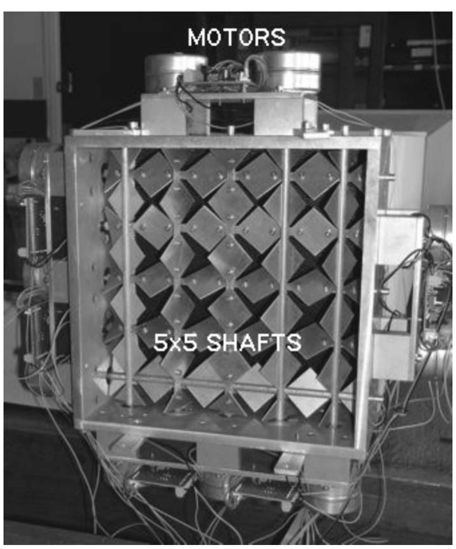

Fig. 2. View of the active grid made of five vertical and five horizontal shafts. Each shaft is fitted with coplanar four square wings and two triangle wings at each end. Each rod is connected to its own stepper motor and control electronics. It is driven by a TTL clock for the step frequency and a TTL signal for the direction of rotation. The frequency and direction are changed randomly in a double random asynchronous mode inspired by Poorte and Biesheuvel (Ref. 3).

Hot wire systems are very valuable tools due to their accuracy, time resolution, and small size (see Ref. 4 for example). The main difficulty is the calibration of the system to determine its nonlinear characteristic $u_x = f(e)$, where e is the output voltage. For simplicity and to avoid manipulation of the wire supporting system (and possibly bad repositioning of the probe), the calibration is performed *in situ*. The active grid is stopped with fully opened blades to ensure that the turbulence level is as small as possible (a few percent). A Pitot probe is positioned next to the hot wire to give a measurement of the average longitudinal flow velocity. The heated wire is positioned vertically, orthogonal to the average flow velocity. The calibration curve is observed to follow the classical King law[4] $e^2 = a\sqrt{u_x} + b$, where a and b are the calibration parameters. The calibration is probably the largest source of measurement error. For example, the longitudinal root mean square (rms) velocity seems to be underestimated by 5% in some cases compared to measurements performed by the laser Doppler velocimetry system. This underestimate may be due to the persistent turbulent fluctuations during the calibration procedure. Ideally the active grid should be removed from the tunnel for calibration, but this removal involves some manipulation of the tunnel, which makes the procedure difficult (especially in the context of a undergraduate lab that is limited in time).

The velocity field of a turbulent flow is a function both of time and space. The hot wire measures the velocity component $u_x(\mathbf{r}_0, t)$ at its fixed position $\mathbf{r}_0$ as a function of time t. The theoretical predictions of the Kolmogorov theory of turbulence concern the spatial variations of the velocity and not the temporal variations. It is possible to relate the temporal fluctuations of the velocity to its spatial fluctuations by using the Taylor hypothesis of frozen turbulence: the velocity fluctuations are advected by the mean flow, which is usually much larger than the velocity fluctuations (see Ref. 5). The sweeping time of a structure of size ℓ is usually much shorter than the typical time scale of the dynamics of the structure: it appears frozen when swept over the probe. A measurement in time is actually a measurement in space in the frame of reference moving with the mean flow $u_x(x, t_0) \approx u_x(x_0, t_0 - x/\bar{u})$ ($\bar{u}$ is the mean velocity). We obtain a one-dimensional cut of the flow.

III. THE 1941 KOLMOGOROV THEORY

A. The Kolmogorov spectrum

For explanations of the Kolmogorov theory and its consequences, the reader should refer to Refs. 1 and 6, or 5 In the following I only give a few relevant results for our analysis.

The most famous prediction of the Kolmogorov theory is the $k^{-5/3}$ evolution of the power spectrum of the velocity fluctuations. Following Pope,[5] we call $E(k)$ the energy spectrum averaged over the orientations of the wave vector $\mathbf{k}$ so that the kinetic energy is

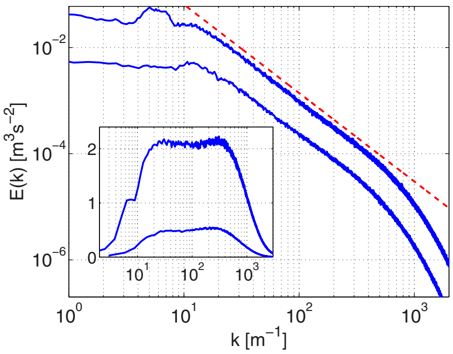

Fig. 3. Velocity spectrum $E(k)$ for an average velocity of 5.7 m/s (upper curve) and 2.5 m/s (lower curve). The probe is located at 80 cm from the grid. The dashed line is a $k^{-5/3}$ decay. The curves are displayed on a log-log scale. The inset is a plot of the spectrum divided by Kolmogorov scaling: $E(k)k^{5/3}$ (semilog scale) with 5.7 m/s (upper curve) and 2.5 m/s (lower curve).

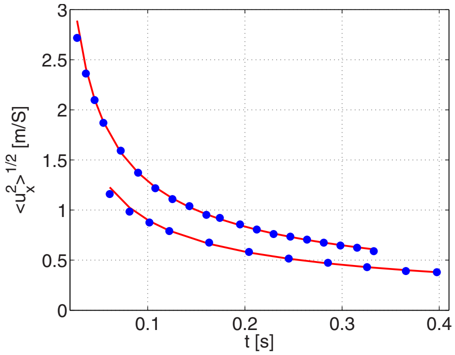

Fig. 4. Decay of the velocity fluctuations for an average velocity of 5.7 m/s (upper circles) and 2.5 m/s (lower circles). The continuous lines are power laws: $0.31t^{-0.62}$ for the upper curve and $0.21t^{-0.62}$ for the lower.

$$\frac{1}{2}\langle \mathbf{u}^2\rangle = \int_0^\infty E(k)\mathrm{d}k. \tag{1}$$

The inertial range is defined as the range of length scales that are much less than the energy injection characteristic scale L, but are much larger than the length scale η for which viscous effects become dominant. Because of the scale separation $2\pi/L \ll k \ll 2\pi/\eta$, $E(k)$ is predicted to depend only on the wave number modulus k and the energy dissipation rate (per unit mass) ϵ for stationary isotropic turbulence. In the inertial range dissipation is negligible and energy is transferred across length scales (or wave numbers). The quantity ϵ is then interpreted as an energy flux across length scales. Dimensional analysis yields

$$E(k) = C\epsilon^{2/3}k^{-5/3}, \tag{2}$$

where C is a universal constant which is empirically estimated to be about 1.5.[5] The hot wire technique allows us to obtain only a one-dimensional measurement and a one-dimensional velocity spectrum. It is possible to show that the one-dimensional spectrum follows the same behavior, the constant C being replaced by $C_1 \approx 0.5$.[5] In the following, we call $E(k)$ the one-dimensional spectrum for simplicity ($\langle u_x^2\rangle = \int_0^\infty E(k)\,\mathrm{d}k$ by definition).

Figure 3 shows an example of a power spectrum measured in our wind tunnel. A very clear $k^{-5/3}$ regime is observed. The inset shows a plot of $k^{5/3}E(k)$ that displays a plateau for about one decade of wave numbers. It is clear that the turbulence level in our grid tunnel is large enough to observe scaling of the power spectrum consistent with Kolmogorov's prediction.

A faster decrease of the spectrum is observed for $k > 400\ \mathrm{m}^{-1}$, corresponding to a cut-off length of about 2.5 mm. This length is larger than the hot-wire length (1.5 mm), so the inertial range is resolved as well as the observed cutoff. The shape of the spectrum for the highest wave numbers, corresponding to length scales smaller than the wire length, is most likely affected by the averaging effect over the length of the probe.

B. The dissipation rate

The Kolmogorov theory involves the quantity ϵ, which is not very intuitive because ϵ appears as an energy flux over wave numbers. We can make the meaning of ϵ more clear by measuring the decay of the energy of the turbulent fluctuations downstream from the active grid. Figure 4 shows the decay of the standard deviation of the velocity as a function of the time of flight from the grid (obtained by using the Taylor hypothesis). After a transition region the decay follows a power law $\langle u_x^2\rangle \propto t^{-m}$. A fit of this power law gives $m \approx 1.24$, which is in the range of values reported in Ref. 3 for various forcing schemes of the active grid. The decay of the energy as a function of the time after its generation by the grid is directly linked to ϵ (assuming isotropy) by

$$\epsilon = -\frac{3}{2}\frac{\mathrm{d}u_x^2}{\mathrm{d}t}. \tag{3}$$

In our case the ratio of the transverse to the longitudinal root mean square velocity is 0.925 over the length of the wind tunnel (as measured by a laser Doppler velocimetry system). The kinetic energy is $1.35u_x^2$ instead of $3u_x^2/2$ for perfect isotropy. Our estimate of ϵ can be compared to that obtained from the Kolmogorov prediction $E(k) = C_1\epsilon^{2/3}k^{-5/3}$.

Another way to estimate ϵ is to use the Kármán-Howarth relation,[5] which can be written in the inertial range and for large Reynolds numbers as

$$\langle (u_x(x+\ell,t) - u_x(x,t))^3\rangle = -\frac{4}{5}\epsilon\ell. \tag{4}$$

The left-hand side of Eq. (4) is the third-order structure function and is displayed in Fig. 5. The structure function is seen to depend linearly on ℓ in the inertial range and gives another estimate of the dissipation rate.

The three estimates of the dissipation rate are given in Table I. The estimates from the spectrum (ϵ_s) and the third order structure function (ϵ_{KH}) are seen to be in good agreement, and the estimate from the energy decay (ϵ) is always higher. The discrepancy seems to increase with the Reynolds number and may be due to a slightly different decay rate of the transverse fluctuations.

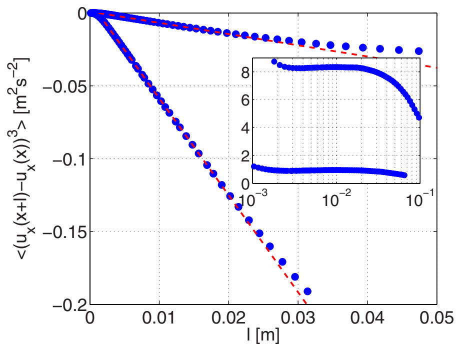

Fig. 5. Third order structure function $S_3(\ell)=\langle(u_x(x+\ell,t)-u_x(x,t))^3\rangle$ as a function of ℓ for an average velocity of 5.7 m/s (lower circles) and 2.5 m/s (upper circles). The dashed lines are linear fits to $a\ell+b$. The insert is a plot of $-(5/4\ell)(S_3(\ell)-b)$ at an average speed of 5.7 m/s (upper circles) and 2.5 m/s (lower circles). The plateau value should be ϵ.

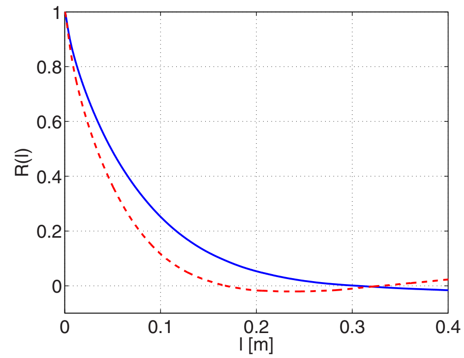

Fig. 6. Autocorrelation coefficient $\langle u_x(x+\ell)u_x(\ell)\rangle/\langle u_x^2\rangle$ for an average velocity of 5.7 m/s (solid line) and 2.5 m/s (dashed line).

C. Characteristic length scales

We estimate some characteristic length scales to better describe the flow. The integral length scale is related to the energy injection in the flow. Intuitively, it is connected to the grid mesh size. To estimate it numerically we compute $L=\int_0^{+\infty}R(\ell)d\ell$ where $R(\ell)=\langle u_x(x+\ell)u_x(\ell)\rangle/\langle u_x^2\rangle$ is the correlation coefficient of the velocity. The correlation is displayed in Fig. 6. We see that it becomes negative for some value because of a slow oscillation that is a temporal trace of the forcing. It is not significant for the integral scale determination so we can restrict the upper limit of the integral to the length at which the correlation is zero. The values of L for various average velocities are given in Table I. We observe that L is of the same order of magnitude as the grid mesh size (5 cm) but slowly increases with the average velocity.

The Kolmogorov length scale can be defined in terms of the dissipation rate as $\eta=(\nu^3/\epsilon)^{1/4}$, where $\nu=1.5\times10^{-5}\ \mathrm{m^2/s}$ is the kinematic viscosity of air. This length scale separates the viscous regime (scales smaller than η) from the inertial range. The values of η are sub-millimeter (see Table I) so that the hot wire cannot resolve the viscous range (its length is 1.5 mm).

The Taylor length scale λ can be defined in terms of the magnitude of the velocity gradients,

$$\left\langle\left(\frac{\partial u_x}{\partial x}\right)^2\right\rangle=\frac{u_{\mathrm{rms}}^2}{\lambda^2}, \tag{5}$$

where u_{rms} is the root mean square average of the velocity fluctuations. Assuming isotropy, the dissipation rate can be rewritten as $\epsilon=15\nu\langle(\partial u_x/\partial x)^2\rangle$ so that $\lambda=\sqrt{15\nu u_{\mathrm{rms}}^2/\epsilon}$; the corresponding values are given in Table I. The length scale λ is typically larger than the wire length so that the measurement of the flow velocity is resolved down to the Taylor length scale. The estimate of the Taylor length scale leads to another estimate of the Reynolds number that is often preferred to the classical Reynolds number $\bar{u}L/\nu$ because of its intrinsic nature (based on fluctuating quantities only):[6]

$$R_\lambda=\frac{u_{\mathrm{rms}}\lambda}{\nu}. \tag{6}$$

R_λ reaches about 300 at maximum speed (see Table I), which is large enough to claim that we are seeing fully developed turbulence.

Knowing these characteristic length scales, the spectra can be replotted in dimensionless versions, that is, by plotting $E(k)/(C_1\epsilon_s^{2/3}\ell^{5/3})$ versus $k\ell$ for $\ell=L$ or $\ell=\eta$ and for two values of the Reynolds number (see Fig. 7). When $\ell=L$, the transitions from the large scale regime to the inertial range are superimposed, confirming that L is characteristic of the energy injection length scale. The cutoff at high wave numbers occurs for larger values for the highest Reynolds number as expected.

When scaled by $\ell=\eta$ (inset of Fig. 7), the spectra are no longer superimposed at large length scales, which is expected because η is characteristic of the viscous length scale. The spectra are also not superimposed at large wave numbers as they should (see Ref. 5 for example). The reason is that our hot wire probe is too long to resolve the viscous scales (the length of the probe is 1.5 mm compared to η, which is less than 0.25 mm). Thus the high wave number decay is impacted by a filtering effect of the probe.

IV. INTERMITTENCY

A. The distribution of velocity increments

The Kolmogorov picture successfully describes the velocity power spectra, but has some limitations, in particular

Table I. The parameters $\bar{u}$ and u_{rms} are the average and rms flow longitudinal velocity at 80 cm from the grid; u_0^2 and m are parameters of the fit of the decay of the velocity fluctuations $u_{\mathrm{rms}}^2=u_0^2t^{-m}$; ϵ, ϵ_s and ϵ_{KH} are estimates of the dissipation rate from the energy decay, the Kolmogorov spectrum, and the Kármán-Howarth relation [Eq. (4)], respectively; λ is the Taylor length scale, R_λ is the Taylor based Reynolds number, and η is the Kolmogorov length.

$\bar{u}$ (m/s)	u_{rms} (m/s)	u_0^2	m	ϵ (W/kg)	ϵ_s (W/kg)	ϵ_{KH} (W/kg)	λ (mm)	R_λ	η (mm)	L (mm)
2.5	0.43	0.046	1.25	0.98	0.96	0.98	6.5	190	0.24	45
3.9	0.69	0.068	1.24	3.9	3.15	3.1	5.2	240	0.17	54
5.7	1.04	0.094	1.25	12.5	8.6	8.3	4.4	300	0.13	68

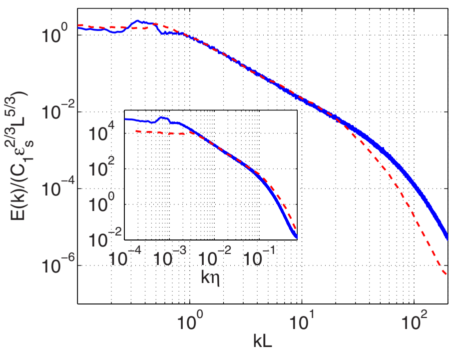

Fig. 7. Normalized spectra $E(k)/(C_1\epsilon^{2/3}\ell^{5/3})$ as a function of $k\ell$ for $\ell = L$, the integral scale, and $\ell = \eta$, the Kolmogorov scale (insert). The spectrum with the narrowest inertial range (dashed line) corresponds to $\bar{u} = 2.5$ m/s and the other to $\bar{u} = 5.7$ m/s (solid line).

when looking at moments that are higher order than quadratic in the velocity. The usual object of analysis is the velocity increment at scale ℓ:

$$\delta_\ell u(x) = u_x(x+\ell) - u_x(x). \tag{7}$$

This velocity difference separated by a distance ℓ is a way to analyze the velocity field in terms of length scales. Note that when ℓ goes to zero $\delta_\ell u \sim \ell du_x/dx$ (assuming that the smallest scales are resolved, which is not really the case here). In the 1941 Kolmogorov theory the velocity field is self-similar on all length scales in the inertial range so that, for example, the distributions of the velocity increments are not expected to depend on the scale ℓ. What is observed in Fig. 8 is a change of the distribution as the scale varies from integral scales down to dissipative ones. For $\ell > L$ the distribution of the increments is Gaussian: $u_x(x+\ell)$ and $u_x(x)$ are uncorrelated for large ℓ so that the distribution of the difference is Gaussian (because the distribution of u_x is also Gaussian). When ℓ is decreased in the inertial range, two effects are observed. First the distribution becomes nonsymmetric: it is negatively skewed as expected from the Kármán-Howarth relation.[6] Second, the tails are observed to become wider as ℓ is decreased, and the shape widens.

These changes can be quantified in terms of the dimensionless skewness,

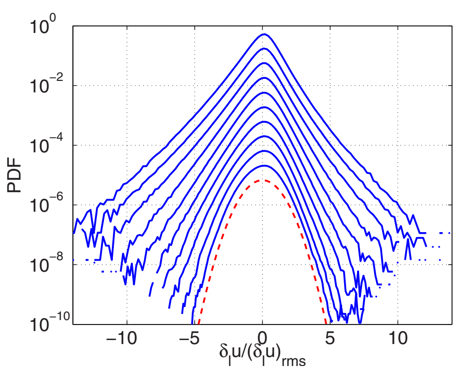

Fig. 8. Probability density of the velocity increments $\delta_\ell u$ for $\ell = 0.3$, 0.6, 1.2, 2.4, 4.8, 9.6, 19, 39, 77, and 155 mm (from top to bottom) for $\bar{u} = 5.7$ m/s at 80 cm from the grid. The curves are vertically shifted from each other by a factor of 2 for clarity. The dashed line is a Gaussian distribution.

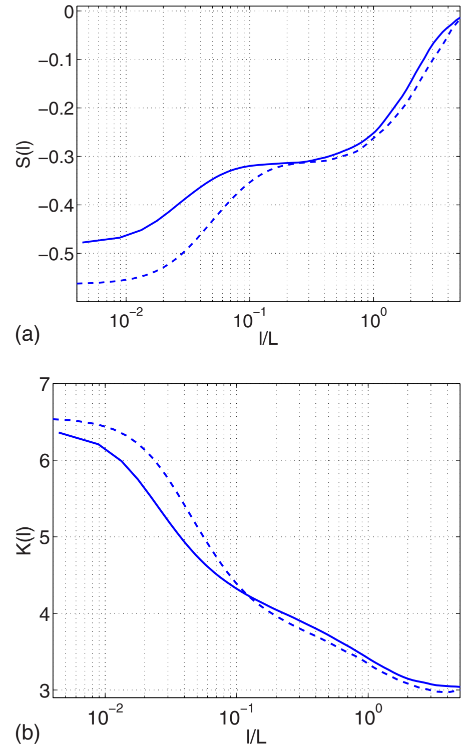

Fig. 9. (a) Skewness $S(\ell)$ and (b) flatness $K(\ell)$ of the velocity increments $\delta_\ell u$ as a function of the scale ℓ for $\bar{u} = 5.7$ m/s (continuous line) and $\bar{u} = 2.5$ m/s (dashed line).

$$S(\ell) = \frac{\langle(\delta_\ell u)^3\rangle}{\langle(\delta_\ell u)^2\rangle^{3/2}}, \tag{8}$$

which is a measure of the asymmetry of the distribution, and the dimensionless flatness,

$$K(\ell) = \frac{\langle(\delta_\ell u)^4\rangle}{\langle(\delta_\ell u)^2\rangle^2}, \tag{9}$$

which is a measure of the width of the tails of the distribution. The average denoted by $\langle \ldots \rangle$ is an average over the statistical realizations of the flow, but here it is taken as an average over x (actually an average over time because of the use of the Taylor hypothesis). Both quantities are displayed in Fig. 9.

The skewness is seen to take a constant value of about -0.31 in the inertial range. The Kolmogorov theory predicts that $\langle(\delta_\ell u)^2\rangle$ should behave like $C_2(\epsilon\ell)^{2/3}$ (with $C_2 \approx 2$).[5] If we use the Kármán-Howarth relation, the skewness is expected to be constant and close to $-4/(5C_2^{3/2}) \approx -0.28$, which is fairly close to what is observed. The skewness can be seen as a measure of the energy flux across length scales due to the dissipation process which acts as an energy sink. The skewness is seen to go to zero at large ℓ/L (compatible with a Gaussian distribution) and become even more negative in the dissipative range. The fact that the value of the skewness for small ℓ is less negative for the highest Reynolds number than for the lowest suggests that the smallest scales are not resolved by the hot wire, and thus the values measured at the smallest scales are not indicative of the actual values.

In contrast to the skewness, the flatness is seen to decrease continuously with ℓ/L and reaches 3 at large scales (the value expected for a Gaussian distribution). It decreases

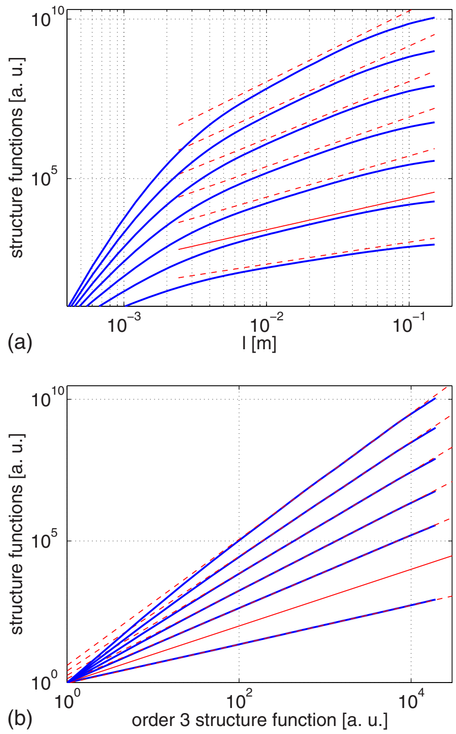

Fig. 10. Structure functions for $\bar{u}=5.7$ m/s. (a) Plot of $S_p(\ell)$ as a function of ℓ for $p=2$, 3, 4, 5, 6, 7, and 8 from bottom to top (the curves are arbitrarily shifted vertically). The solid line depends linearly on ℓ. The dashed lines are power laws of exponents ξ_p (see text). (b) An extended self-similarity plot of S_p for $p=2$, 4, 5, 6, 7, and 8 as a function of S_3. The continuous straight line is S_3. The dashed lines are power laws that determine ξ_p: $S_p \propto S_3^{\xi_p}$.

slowly with ℓ/L in the inertial range. From the measured intermittency exponents (see the following), it is expected to decrease as a power law with the exponent -0.1. The decrease accelerates abruptly in the near dissipative range (as is well documented, for example, in Ref. 7). The observed continuous change with ℓ, in particular in the inertial range, means that the statistics of the velocity increments are not self-similar in contrast with the predictions of the Kolmogorov theory, and thus they display more complex statistics.

B. Structure functions

One way to describe more accurately the velocity increment distribution is to study the successive moments as a function of the length scale ℓ. These are the structure functions defined as

$$S_p(\ell) = \langle(|\delta_\ell u|)^p\rangle. \tag{10}$$

We use absolute values to eliminate the asymmetry effects. The structure functions are displayed in Fig. 10. The structure functions are expected to behave as $S_p \propto \ell^{\zeta_p}$. Here the Reynolds number is not very high so that the power law scaling is far from perfect. A fit of the form $S_p(\ell)=a\ell^{\zeta_p}+b$ gives better agreement than a simple power law. S_p is commonly displayed as a function of S_3, which is expected to behave linearly in ℓ in the inertial range.[6] We observe that the scaling $S_p \propto S_3^{\xi_p}$ looks more convincing than the scaling $S_p(\ell) \sim \ell^{\zeta_p}$. For true scaling as a function of the length scale, we have $\xi_p=\zeta_p$ if $\zeta_3=1$ as expected dimensionally from the Kolmogorov theory (the Kármán-Howarth relation does not give the scaling of S_3 because absolute values are used).

Table II. Exponents of the observed power law behaviors: $S_p \propto S_3^{\xi_p}$ (see text and Fig. 10).

$\bar{u}$	p	2	3	4	5	6	7	8
2.5	ξ_p	0.69	1	1.29	1.55	1.80	2.02	2.22
3.9	ξ_p	0.69	1	1.28	1.55	1.79	2.02	2.23
5.7	ξ_p	0.69	1	1.28	1.54	1.78	2.00	2.21
	from Ref. 6	0.70	1	1.28	1.53	1.77	2.01	2.23
	Kolmogorov	2/3	1	4/3	5/3	2	7/3	8/3

What is also observed is that the exponents ξ_p (given in Table II) display the same values as are measured at higher Reynolds numbers.

The Kolmogorov theory predicts that the exponents ζ_p take the value $p/3$. We see that the measured values clearly deviate from the Kolmogorov prediction. This phenomenon is called intermittency (see Ref. 6). For $p>3$ we obtain $\xi_p < p/3$. ξ_2 takes the value 0.69, which differs slightly from 2/3 (the measured difference is meaningful). This difference means that the Kolmogorov spectrum is expected to deviate slightly from the $k^{-5/3}$ scaling. The observation of this discrepancy requires a very accurate measurement. The product $E(k)k^{5/3}$ in the insert of Fig. 3 is slightly decreasing; the product $E(k)k^{1.69}$ looks more horizontal (not shown). A higher Reynolds number experiment is required to discriminate between a genuine effect or a finite Reynolds number effect. Intermittency is still an active field of research.[8–10]

V. CONCLUSIONS

Our wind tunnel allows us to observe features related to high Reynolds number turbulence such as the Kolmogorov $k^{-5/3}$ spectrum and the Kármán-Howarth relation related to the skewness of the velocity derivative. We also can discuss the various relevant length scales of the flow. The Reynolds number is high enough to quantify deviations from the Kolmogorov theory and observe intermittency phenomenon. We also can discuss the limitations of our measurements, which has pedagogical value. The wind tunnel introduces digital data acquisition and processing such as the fast Fourier transform and digital filtering. The wind tunnel has further advantages from a teaching point of view, namely its moderate size and its moderate price,[11] and opens many possibilities to introduce undergraduate students to fluid turbulence.

ACKNOWLEDGMENTS

I would like to gratefully thank the Physics Department of the Ecole Normale Supérieure for supporting this work and giving me the opportunity to build the teaching wind tunnel. I thank François Daviaud from CEA Saclay for allowing me to use his Laser Doppler Velocimetry system. I am grateful to Jose Quintas Da Silva for technical advice on the machining of the active grid. I also thank Romain Bassez who was the first student to extensively test this device.

[a]Electronic mail: nmordant@ens.fr

[1]Mark Nelkin, "Resource Letter TF-1: Turbulence in fluids," Am. J. Phys. **68**(4), 310–318 (2000).
[2]Hideharu Makita, "Realization of a large-scale turbulence field in a small wind tunnel," Fluid Dyn. Res. **8**, 53–64 (1991).
[3]R. E. G. Poorte and A. Biesheuvel, "Experiments on the motion of gas

bubbles in turbulence generated by an active grid," J. Fluid Mech. **461**, 127–154 (2002).
[4]H. H. Bruun, *Hot-Wire Anemometry* (Oxford U. P., Oxford, 1995).
[5]Stephen B. Pope, *Turbulent Flows* (Cambridge U. P., Cambridge, 2000).
[6]Uriel Frisch, *Turbulence, The Legacy of A. N. Kolmogorov* (Cambridge U. P., Cambridge, 1995).
[7]Laurent Chevillard, Bernard Castaing, and Emmanuel Lévêque, "On the rapid increase of intermittency in the near-dissipation range of fully developed turbulence," Eur. Phys. J. B **45**, 561–567 (2005).
[8]A. Arnéodo *et al.*, "Universal intermittent properties of particle trajectories in highly turbulent flows," Phys. Rev. Lett. **100**, 254504-1–4 (2008).
[9]A. Gylfason and Z. Warhaft, "On higher order passive scalar structure functions in grid turbulence," Phys. Fluids **16**(11), 4012–4019 (2004).
[10]Focus issue on turbulence, New J. Phys. **6** (2004).
[11]The four fans cost about 80€ each, the stepper motors are 45€ each with their controller. The wood, honeycomb, and machining may total about 1000 euros (and some time). The most expensive part is the instrumentation, hot wire, and Pitot probe systems, which are a couple of thousand euros each. The digital signal acquisition boards are most likely available in the laboratory and otherwise cost about 1000 euros each.

Lens Set. These three lenses are in regular use in lecture demonstrations at the University of Cincinnati physics department. The sheet brass outlines show that the lenses are double-convex (converging), plano-convex (converging) and double-concave (diverging). The set is marked Jules Duboscq/Ph PELLIN/Paris. Jules Duboscq (1817–1886) was succeeded in business by Phillippe Pellin. (Photograph and Notes by Thomas B. Greenslade, Jr., Kenyon College)